NETWORK DYNAMICS AND CELL PHYSIOLOGY

John J. Tyson*, Kathy Chen* and Bela Novak‡

Complex assemblies of interacting proteins carry out most of the interesting jobs in a cell, such as metabolism, DNA synthesis, movement and information processing. These physiological properties play out as a subtle molecular dance, choreographed by underlying regulatory networks. To understand this dance, a new breed of theoretical molecular biologists reproduces these networks in computers and in the mathematical language of dynamical systems.

MILESTONES

The ultimate goal of molecular cell biology is to understand the physiology of living cells in terms of the information that is encoded in the genome of the cell. Everyone is aware of the broad outline of this enterprise (FIG. 1) — nucleotide sequences are translated into amino-acid sequences, and the linear sequence of amino acids directs the folding of a protein into its native three-dimensional shape. That shape, in turn, determines the functional properties of the protein. Individual proteins carry out their function in complex networks of interacting macromolecules, the coordinated behaviour of which determines the physiological properties of the living cell.

In recent years, it has become increasingly clear that sophisticated computational methods will be needed to manage, interpret and understand the complexity of biological information. The analysis of nucleotide strings — to assemble genomic sequences and to identify protein-coding regions — is already big business. Database services, such as multiple sequence alignments, are now familiar computational tools that are easily used by experimentalists. Conversely, the prediction of protein structure from primary sequence, despite its urgency, is not so easy[1,2]. Many scientific and computational problems remain to be solved before protein-structure prediction becomes a reliable and readily available tool.

The next level of organization — predicting protein function from structure — involves new theoretical challenges. Useful tools exist to predict protein–ligand binding, based on molecular dynamics simulations[3,4].

Sophisticated methods, based on quantum mechanics, statistical mechanics and electrostatics, have been used to understand diverse protein-mediated processes, such as photosynthetic light absorption[5], ATP synthesis[6] and ion transport[7].

Even if we could predict the physicochemical properties (binding constants, rate constants, transport coefficients and so on) of a protein from its three-dimensional structure, we would still be in the dark about the properties of the networks in which individual proteins operate. If it were necessary, in a single model, to span

*Department of Biology, Virginia Polytechnic Institute and State University, Blacksburg, Virginia 24061, USA. ‡Department of Agricultural Chemical Technology, Budapest University of Technology and Economics, Budapest 1521, Hungary. Correspondence to J.J.T. e-mails: tyson@vt.edu, kchen@vt.edu, bnovak@chem.bme.hu
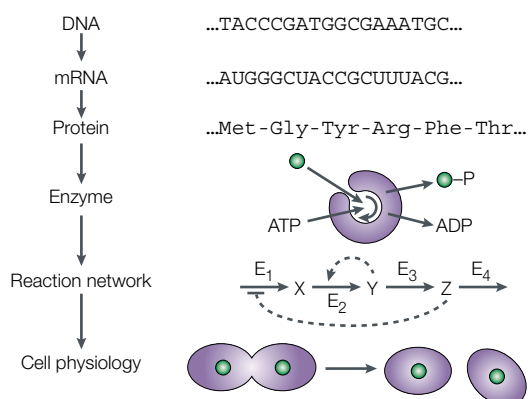
Figure 1 | **Computational molecular biology.** Each step in the flow of information from nucleotide sequences to cell physiology entails sophisticated computational challenges, such as sequence analysis, protein folding and the dynamical behaviour of molecular regulatory systems.

Box 1 | **Recent calls for a theory to connect network dynamics to cell physiology**

• Fraser and Harland (2000)[59]

"[R]esults to date show a dizzying array of signalling systems acting within and between cells. …In such settings, intuition can be inadequate, often giving incomplete or incorrect predictions. …In the face of such complexity, computational tools must be employed as a tool for understanding."

• Nurse (2000)[60]

"Perhaps a proper understanding of the complex regulatory networks making up cellular systems like the cell cycle will require a …shift from common sense thinking. We might need to move into a strange more abstract world, more readily analyzable in terms of mathematics than our present imaginings of cells operating as a microcosm of our everyday world."

• Hartwell, Hopfield, Leibler and Murray (1999)[61]

"The best test of our understanding of cells will be to make quantitative predictions about their behaviour and test them. This will require detailed simulations of the biochemical processes taking place within [cells]. …We need to develop simplifying, higher-level models and find general principles that will allow us to grasp and manipulate the functions of [biochemical networks]."

• Venter (1999), as quoted in Butler[62]

"If we hope to understand biology, instead of looking at one little protein at a time, which is not how biology works, we will need to understand the integration of thousands of proteins in a dynamically changing environment. A computer will be the biologist's number one tool."

all the scales in FIG. 1 — from molecular motions (nanometres and picoseconds) to cell responses (micrometres and seconds, or longer) — then a theoretical approach to cell biology would be beyond our grasp, both computationally and intellectually. Fortunately, considerable progress can be made at any given level of the hierarchy, independently of the successes or failures at levels both above and below.

In this review, we concentrate on the last step in FIG. 1 — derivation of the physiological properties of a cell from the wiring diagrams of its control systems. These networks of interacting proteins are intrinsically dynamic: they describe how a cell changes in space and time to respond to stimuli, grow and reproduce, differ-

entiate, and do all the other remarkable tricks that are necessary to stay alive and perpetuate the species. In the past year, many prominent molecular biologists have pointed out the pressing need for theoretical and computational tools to show the spatial and temporal organization implicit in the way that macromolecules are 'wired together' to create a living cell (BOX 1).

Of special significance are the regulatory pathways that control cell behaviour, because these pathways are the 'brains' of the cell[8]. They receive information from outside and inside the cell by signal-transduction pathways, process the information to make 'decisions', then trigger responses that are appropriate to the survival and reproduction of the cell. For instance, a fibroblast cell, after processing information about growth factors in its environment and its state of attachment to the extracellular matrix and neighbouring cells, might make a decision to proliferate. In that case, it downregulates the retinoblastoma protein, which allows the cell to grow, replicate its DNA and divide[9,10]. The molecular signals that control the proliferation of mammalian cells are extremely complex[11], and Kohn's map[12] of this network has become an icon of the challenges that confront any attempt to fathom a realistic cellular control system.

What tools do we have to help us understand how the precise spatio-temporal organization of a cell arises from the molecular interactions of the protein machinery inside? Are there ways to compute physiology from network topology? And is there a solid theoretical foundation for such computations?

The cell is a dynamical system

The capacity of a cell to change in space and time is crucial to survival and reproduction. The dynamical properties of a cell are implicit in the topology of the protein networks that underlie cell physiology. For example, in BOX 2, we describe the basic network that controls cell division in the fission yeast *Schizosaccharomyces pombe*.
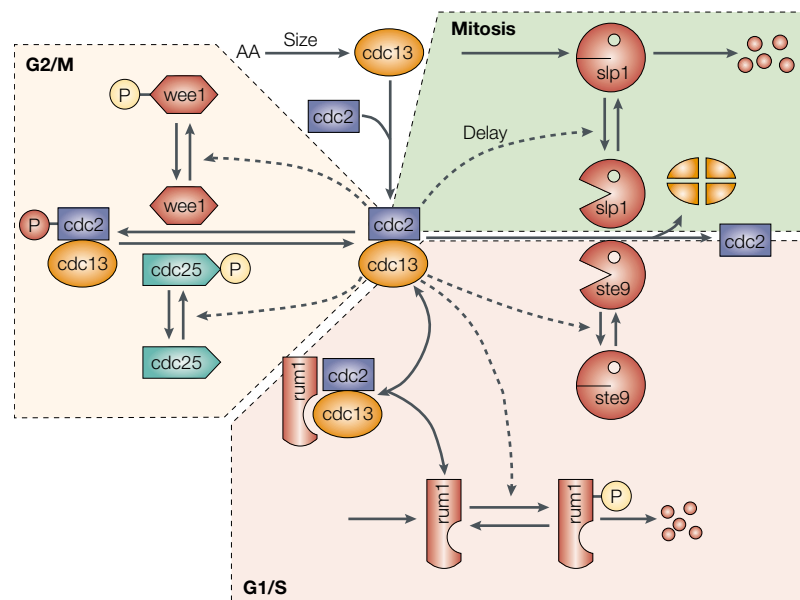

Figure 2 | **The cell-cycle control system in fission yeast.** This system can be divided into three modules, which regulate the transitions from G1 into S phase, from G2 into M phase, and exit from mitosis. BOX 2 describes in more detail the proteins and interactions involved.

The wiring diagram (FIG. 2) implies a set of dynamical relationships among its components and, therefore, demands to be converted into a set of mathematical equations that describe the temporal and spatial evolution of the system.

The type of equations to be used depends on the biological questions under consideration[13]. For instance, genetic regulatory circuits might be modelled by differential equations or by Boolean networks[14–18]. Spatial signalling might be modelled by partial differential equations or by cellular automata[19–22]. Functional or integro-differential equations are called for when signif-icant time delays enter the process[23–25], or when spatial averaging is involved[26,27]. When small numbers of mole-cules are involved, stochastic models must be used[28,29].

For the cell-cycle control system, it is appropriate to use ordinary differential equations (ODEs), because molecular diffusion, transcription, translation and membrane transport seem to be fast (a matter of seconds) compared with the duration of the cell cycle (hours). Spatial localization of reactions can be handled by compartmental modelling, in the spirit of pharma-cokinetics[30]. The differential equations used (BOX 2) sim-ply capture, in mathematical terms, our intuitive ideas

---

Box 2 | Cell-cycle regulation in fission yeast

The molecular machinery that regulates cell division in fission yeast is represented in FIG. 2 as a biochemical 'wiring diagram' (REFS 45,63). Each node represents a specific protein; the arrows coming into (or going out of) a node repre-sent the processes that produce or activate (or consume or inactivate) that protein. Furthermore, the proteins affect each other's dynamics not only as substrates and products, but also as regulators of biochemical conversions (the dashed arrows from nodes to reactions).

Major events of the cell cycle in fission yeast are triggered by a CYCLIN-DEPENDENT KINASE (cdc2) in association with a B-TYPE CYCLIN (cdc13). (These proteins are known by different names in other organisms, as summarized in TABLE 1.) The control system can be divided into three modules. The first module regulates the transition from G1 into S phase. Cdc2–cdc13 dimers are in short supply in G1 because cdc13 is rapidly degraded by ste9. (More precisely, ste9 targets cdc13 for UBIQUITYLATION by the ANAPHASE-PROMOTING COMPLEX and subsequent degradation by proteasomes.) In addition, any dimers that might be present are bound to a stoichiometric inhibitor, rum1. Active cdc2–cdc13 opposes its 'enemies' (ste9 and rum1) by phosphorylating them[64–66].

At the G1/S transition, the balance of power shifts from ste9 and rum1 to cdc2–cdc13. However, cdc13-dependent kinase activity increases only to a moderate level because a second control module (G2/M) comes into play: a tyro-sine kinase, wee1, phosphorylates cdc2, thereby suppressing cdc2–cdc13 activity below the level necessary for initiat-ing mitosis. At the G2/M transition, a tyrosine phosphatase, cdc25, reverses this phosphorylation and promotes entry into mitosis.

Notice that cdc2–cdc13 inhibits wee1 (REF. 67) and activates cdc25 (REF. 68); these positive-feedback loops make for an abrupt transition from G2 into M phase. Exit from mitosis is the job of the third module. As chromosomes align on the metaphase plate, slp1 is activated. Slp1 promotes sister-chromatid separation (anaphase) and degradation of cdc13 (which allows nuclear division and cell division). As cdc2–cdc13 activity drops, the kinase enemies ste9 and rum1 return, and slp1 becomes inactive. The newborn cells are now back in G1 phase, ready to repeat the process.

In the same way that an electrical engineer would convert a wiring diagram into a set of differential equations for electrical currents through the circuits, a biochemist could convert this molecular wiring diagram into a set of differ-ential equations for material currents through the reaction pathways. For instance, we could start to formulate a mathematical description of this control system with rate equations for cdc2–cdc13 and rum1, as follows:

$$\mathrm{d/d}t\,[\mathrm{cdc2\text{-}cdc13}] = k_1 \cdot \mathrm{size} - k_2[\mathrm{cdc2\text{-}cdc13}] - k_3[\mathrm{rum1}][\mathrm{cdc2\text{-}cdc13}] + k_4[\mathrm{rum1\text{-}cdc2\text{-}cdc13}] - k_5[\mathrm{cdc2\text{-}cdc13}] + k_6[\mathrm{cdc2P\text{-}cdc13}]$$

$$\mathrm{d/d}t\,[\mathrm{rum1}] = -k_3[\mathrm{rum1}][\mathrm{cdc2\text{-}cdc13}] + k_4[\mathrm{rum1\text{-}cdc2\text{-}cdc13}] + k_7 - k_8[\mathrm{rum1}] + k_9[\mathrm{rum1P}]$$

The time-rate-of-change of concentration of a component is written as a sum of terms that represent the rate of each reaction (solid line) leading to or from that component in the wiring diagram. To couple the dynamics of cdc2–cdc13 to cell growth and division, we assume that cdc13 is synthesized in the cytoplasm at a rate proportional to ribosome number, then combines with cdc2 (present in excess), and the dimers are sequestered in the nucleus (whose volume, we assume, changes little during the cell cycle). Hence, the rate of increase of nuclear concentration of cdc2–cdc13 is k_1·size, where size is proportional to the number of ribosomes per nucleus. Size increases steadily as the cell grows and drops by a factor of two at cell division. k_2 is the specific rate of degradation of cdc13 (dependent on the activities of slp1 and ste9). k_3 is the rate of trimer formation, and k_4 of trimer dissociation. k_5, which depends on wee1 activity, is the specific rate of phosphorylation of cdc2 subunits, and k_6 describes the phosphatase activity of cdc25. k_7 is the rate of synthesis of rum1, k_8 its rate of phosphorylation (dependent on the activity of cdc2–cdc13). k_9 reflects a phosphatase activity that rescues rum1. Similar equations must be written for each temporally varying pro-tein in the reaction mechanism.

The wiring diagram in this box is described by a dozen differential equations, involving ~30 kinetic parameters. After assigning values to these constants, we can solve the differential equations to produce a simulation of progres-sion through the cell cycle in fission yeast (FIG. 3). The trick is to find a parameter set that accounts not only for the properties of wild-type cells, but also for the phenotypes of mutants that have been constructed by knocking out and overexpressing genes for this protein network.
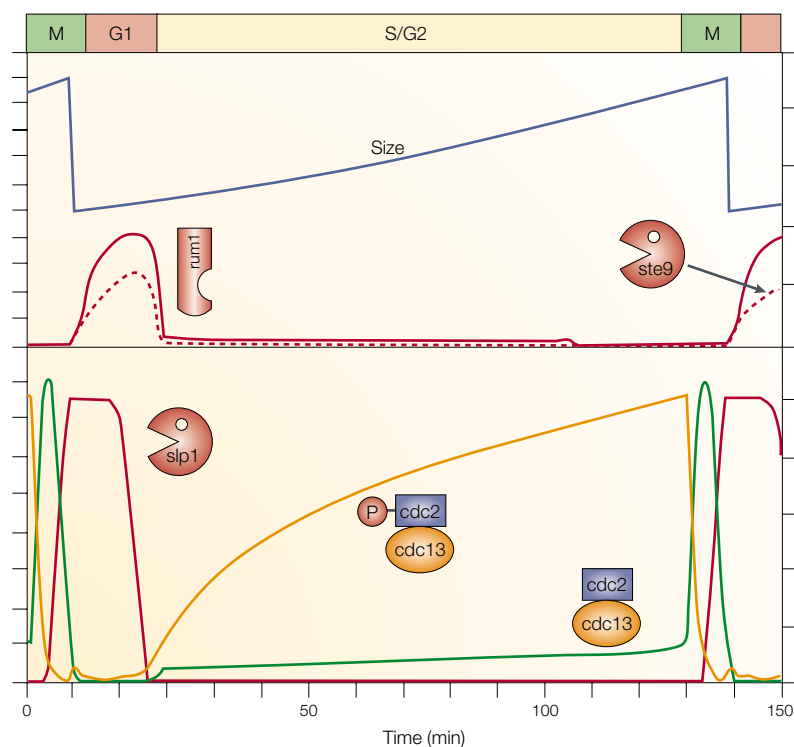

Figure 3 | **Simulated time courses of cdc2 and related proteins during the cell cycle of fission yeast.** Numerical integration of the full set of differential equations that describe the wiring diagram in FIG. 2 yields these time courses. Time is expressed in minutes; all other variables are given in arbitrary units. 'Size' refers to the number of ribosomes per nucleus. Notice the brief G1 phase, when ste9 is active and rum1 is abundant. After a long S/G2 phase, during which cdc2 is tyrosine phosphorylated, the cell enters M phase, when cdc25 removes the inhibitory phosphate group. After some delay, slp1 activates and degrades cdc13. As cdc2–cdc13 activity falls, the cell exits mitosis. Size decreases twofold at nuclear division.

DYNAMICAL SYSTEM
A collection of components (for example, genes, proteins and metabolites) the properties of which change in time of response to interactions among the components and influences from outside the system.

STATE (SPACE)
The set of numbers that quantify each component (state variable) of a dynamical system. If there are n components, then the state can be represented by a point in an n-dimensional state space.

VECTOR FIELD
Assigned to each point in state space is a vector that specifies the magnitude and direction in which the state variables are changing.

STABLE (UNSTABLE)
Refers to steady states or limit cycles that attract (repel) nearby orbits.

about protein synthesis and degradation, phosphorylation and dephosphorylation. They allow us to test a hypothesis (for example, the network in FIG. 2) by computing how the concentration of each protein will rise and fall, and then comparing the simulated behaviour of the model with the observed behaviour of the cell. For the remainder of this article, we focus on ODE models of cell-cycle control to illustrate how cells might be viewed as DYNAMICAL SYSTEMS. For other approaches, see REFS 13–29.

From a mathematical point of view, the STATE of a dynamical system is specified, at any instant of time, by the values of the concentrations of all biochemical species in the reaction network. The differential equations then predict how fast each component changes with time. The equations do not directly tell us the state, but rather how a given state will change over the next small interval of time. To predict the temporal progression of each component, we must integrate the differential equations. Computers excel at this sort of calculation (FIG. 3). Can we just relegate all these problems to our silicon servants?

Even a modest regulatory network, such as that in FIG. 2, requires a large number of differential equations for its description. Before the computer can integrate these equations, we must specify the many

rate constants (the k_is) that appear in the rate laws, but many of these rate constants are unmeasured. If we blindly twiddle rate constants, we might never stumble on a combination that reproduces all the idiosyncracies of how yeast cells grow and divide (including the phenotypes of mutants that can be constructed by knocking out and overexpressing all the components of the network, both singly and in combination). Even if an ideal parameter set was provided (say, by software for automatic parameter optimization), the numerical solutions churned out by the computer would be just as inscrutable as the cell itself. In any case, we need a more intuitive, but still reliable, approach to the solution of differential equations. We need insight into why a control system behaves the way it does, and how this behaviour depends on parameter values. With such insight we have a better chance of developing well-parameterized models that achieve both goals of Hartwell, Hopfield, Leibler and Murray (BOX 1): 'quantitative predictions' and 'general principles'.

Are there general principles and useful tools to sort out the complex behaviour of realistic models of molecular regulatory networks?

Vector fields
The rate equations of a network tell us not "where we are" but "where we are going". Given a location in state space, the rate equations tell us by how much each concentration will change in the next small increment of time. In abstract terms, the kinetic equations define a VECTOR FIELD in state space (FIG. 4). The vector field determines completely the temporal behaviour of the control system, and therefore the physiological behaviour of the cell function being controlled. The vector field points to certain attractors; that is, STABLE solutions of the kinetic equations. For example, in FIG. 4, the control system has two stable STEADY STATES (attractors), which are separated by an unstable SADDLE POINT (a repeller). In some cases, the attractor might be a closed ORBIT in state space (a limit cycle). Attractors of the vector field represent observable physiological states of the control system. We associate stable steady states with CHECKPOINTS in the cell cycle (for example, the G1-arrested state of starving yeast cells). We associate stable limit cycles with sustained oscillations in cyclin-dependent kinase activity (for example, the rapid mitotic cycles of early frog embryos). Even the unstable saddle point, although it cannot be observed directly, has significant physiological consequences, as we shall see.

From a dynamical perspective, the vector field is the connection between molecular machinery (wiring diagrams) and cell physiology: network → vector field → physiology. To understand the origin and implications of the vector field is to understand the physiological potential of the regulatory network[31,32].

Although the geometrical idea of a vector field is intuitively appealing, we immediately bump into a problem. For a simple, two-component mechanism we can draw the vector field as in FIG. 4. But how do we visualize the 12-dimensional vector field that is defined by the complete regulatory system in FIG. 2? To get around

Figure 4 | **A vector field.** If, for the sake of illustration, we consider only changes in [cdc2–cdc13] and [rum1], we can characterize the G1/S module in FIG. 2 by a two-dimensional state space. Each point (*x,y*) in the plane corresponds to a possible state (*x* = [rum1], *y* = [cdc2–cdc13]) of the subsystem. At any given point, the differential equations (BOX 2) determine how fast the state of the system is changing; therefore, they associate to each point an arrow , which indicates the direction and magnitude of the rates of change of [cdc2–cdc13] and [rum1]. The collection of arrows at every point in state space defines the vector field of the dynamical system. In this figure, the arrows indicate direction only; magnitude is encoded in colour: red, fast; blue, slow. We have also plotted two curves (solid white lines) on which the vector field is either horizontal or vertical. Within the regions bounded by these curves, all arrows lie in the same quadrant of compass directions. Where the curves intersect, we have steady-state solutions (neither [cdc2–cdc13] nor [rum1] change with time). Knowing the vector field, one can predict the response of the control system to any initial condition; simply pick a starting point and follow the arrows. In this case, the dynamical system has two attractors (●): one with lots of rum1 and little active cdc2–cdc13; and one with little rum1 and lots of cdc2–cdc13. (Notice that, in the vicinity of a stable steady state, all arrows point towards the steady state.) The intermediate steady state (o) is an unstable saddle point (attractive in two directions and repelling in all others). The state-space idea is readily generalized to any number of dynamical variables, but the vector field is hard to visualize in three- (or higher) dimensional state space.
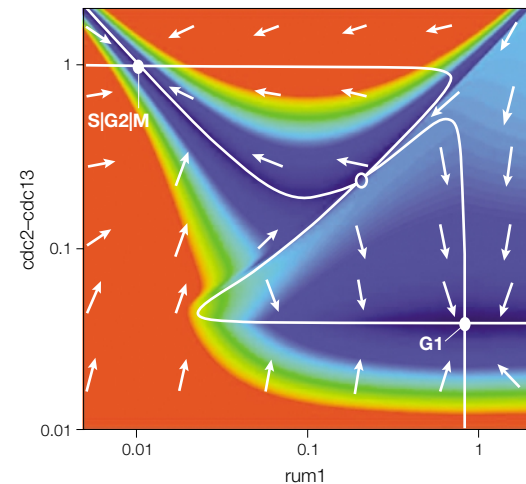
this problem, we need some powerful mathematical tools. These tools are to the theoretical molecular biologist what gel electrophoresis and gene knockouts are to the experimental molecular biologist.

Dynamical systems theory

The perfect tool for this problem is BIFURCATION theory, which tells us how the generic properties of a dynamical system depend on parameter values. Here, we describe the basic idea (for more details, see REFS 33,34). The behaviour of a regulatory network is characterized by the attractors of its vector field in a multidimensional state space that we cannot visualize. The nature of these attractors is determined by parameter values that are chosen from a multidimensional PARAMETER SPACE that might be enormously large. Nonetheless, bifurcation theory assures us that there is only a limited number of ways in which these attractors might transmute as we move continuously through parameter space. For example, a stable steady state might disappear and be replaced by a stable limit cycle, as happens at fertilization in a frog egg, when a metaphase-arrested oocyte transforms into

a rapidly dividing embryo. Bifurcation theory provides a tool — theoretically rigorous and computationally convenient — for finding particular parameter combinations at which these transmutations occur.

Furthermore, these transmutations can be visualized by choosing a single variable as being representative of all the interacting proteins in the network, and a single parameter as representative of all the rate constants that are involved in these reactions. By plotting the proxy variable against the proxy parameter (a bifurcation diagram), we get a visual representation of the behaviour of the dynamical system in dependence on its parameters.

In FIG. 5, we draw bifurcation diagrams for the three modules that comprise the cell-cycle control system in fission yeast (FIG. 2). The G1/S module is a bistable switch (FIG. 5a; also see FIG. 4). For intermediate values of cell size (the number of ribosomes per nucleus), the module has two stable steady states (G1 and S/G2/M), which are separated by an unstable saddle point. As a consequence, a cell of intermediate size might be either in G1 phase (cdc2 activity very low) or in S/G2/M phase (cdc2 activity high). Bistability is a result of the

STEADY STATE
A point in state space where the vector field vanishes (that is, a point that does not move).

SADDLE POINT
A steady state that attracts some nearby orbits and repels others.

ORBIT
A path through state space, traversed over time, as a dynamical system follows the underlying vector field from an initial state to a final state.

CHECKPOINT
A waiting state of the cell-cycle control system, induced by specific conditions such as DNA damage or spindle abnormalities.

BIFURCATION
A combination of parameter values at which something unusual happens to the attractors of a dynamical system; for example, two steady states annihilate each other, or a stable steady state gives way to a stable limit cycle.
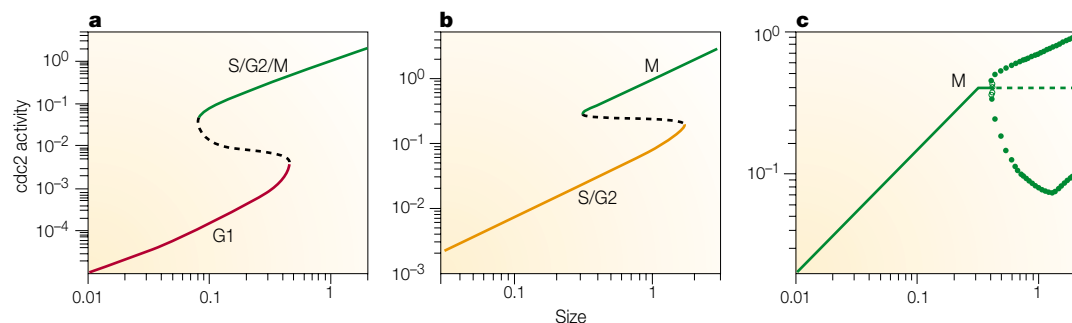

Figure 5 | **Bifurcation diagrams for the three control modules of the cell cycle.** The activity of cdc2–cdc13 dimers (an indicator of the state of the control system) is plotted against 'size' (the number of ribosomes per nucleus, an indicator of cell growth and division). All variables are expressed in arbitrary units. For each value of size, we compute the steady-state activity of cdc2–cdc13. Solid line, stable steady state; dashed line, unstable steady state; solid circles, maximum and minimum excursions around a stable limit cycle; open circles, unstable limit cycle. **a** | The G1/S module. For 0.08 < size < 0.5, the module has two stable steady states (G1, red; S/G2/M, green), which are separated by an unstable saddle point (dashed). **b** | The G2/M module. For 0.3 < size < 1.05, an S/G2 state (orange) coexists with an M state (green). **c** | The mitosis module. The mitotic steady state (green line) loses stability at size = 0.5 (solid line becomes dashed). Stable limit cycles surround the unstable steady state.

Table 1 | Proteins that regulate the eukaryotic cell cycle

Fission yeast	Budding yeast	Frog egg	Mammal	Generic role
cdc2	Cdc28	Cdk1,2	Cdk1,2	Cyclin-dependent kinase
cdc13	Clb1–6	Cyclin A,B,E	Cyclin A,B,E	Cyclins
rum1	Sic1	Xic1	p27^{Kip1}	Stoichiometric inhibitor
ste9	Cdh1	Fizzy-related	Cdh1	APC auxiliary
slp1	Cdc20	Fizzy	p55^{cdc}	APC auxiliary
wee1	Swe1	Wee1	Wee1	Tyrosine kinase
cdc25	Mih1	Cdc25C	Cdc25C	Tyrosine phosphatase

antagonism between cdc2–cdc13 and its enemies, rum1 and ste9. (The roles of these proteins are explained in BOX 2, and their aliases in other organisms are given in TABLE 1.)

If rum1 and ste9 gain the upper hand, then the cell is attracted to the stable G1 steady state. If cdc2–cdc13 gains the upper hand, then the cell flips into the S/G2/M state. At larger cell size (0.45 in FIG. 5a), the G1 steady state fuses with the saddle point and disappears: the G1 state is lost (rum1 and ste9 are turned off), and the cell enters S phase. (Mathematicians call this transition a 'saddle-node bifurcation'; physiologists call it 'Start'.) Notice that the decision of the cell to enter S phase is not easily reversed — small fluctuations in cell size will not flip the control system back to G1. From this point of view, irreversibility of the Start transition is intimately connected to the existence of the unstable, unobservable

saddle point. The connection between saddle-node bifurcations and cell-cycle transitions was first emphasized in REFS 35,36.

The G2/M module is also a bistable switch (FIG. 5b): an S/G2 state is separated from an M state by an unstable saddle point. Bistability in this module results from cdc2–cdc13 inactivating its enemy (wee1) and activating its friend (cdc25). The transition from G2 phase into mitosis is driven by growth: when cell size reaches 1.8 (in FIG. 5b), the stable G2 steady state is lost by a saddle-node bifurcation, and the control system flips irreversibly into M phase. In molecular terms, at this transition, wee1 is inactivated and cdc25 is activated, cdc2 is dephosphorylated at Tyr15, the activity of cdc2–cdc13 increases abruptly, and the mitotic machinery is put into action. The mathematical model[37] recapitulates exactly the sequence of events that was painstakingly uncovered by Paul Nurse and his collaborators in the 1970s and 1980s[38–41].

The mitosis module behaves differently (FIG. 5c): at large size, the mitotic steady state loses stability and stable limit cycles are born. In our model (BOX 2), these oscillations are generated by a negative-feedback loop. Synthesis of cdc13 causes cdc2 activity to build up. After a certain time delay, cdc2–cdc13 activates slp1, which then destroys cdc13. Some time after cdc2 loses its partner, slp1 reverts to its inactive form. Therefore, cdc13 re-accumulates and the process repeats itself. The propensity of the mitosis module for spontaneous, limit-cycle oscillations was first noticed by Albert Goldbeter[42].

Bifurcations underlie cell-cycle transitions

By putting together the bifurcation diagrams of these three modules, we get a new and informative picture of cell-cycle control in fission yeast (FIG. 6). For a very small cell (say, a germinating spore), there is only one stable attractor — a steady state with very low cdc2 activity. This steady state corresponds to the G1 phase of the cell cycle. Cdc2 activity is low because its cyclin partner (cdc13) is being rapidly degraded (ste9 is active) and a stoichiometric inhibitor (rum1) is abundant.

As the cell grows beyond size ~0.3, there arise two new, stable attractors of the vector field: a stable S/G2 state (solid orange line in FIG. 6) with modest kinase activity, and a stable mitotic state (solid green line in FIG. 6) with high kinase activity. Nonetheless, the control system remains in G1 (the red line), because the G1 state is
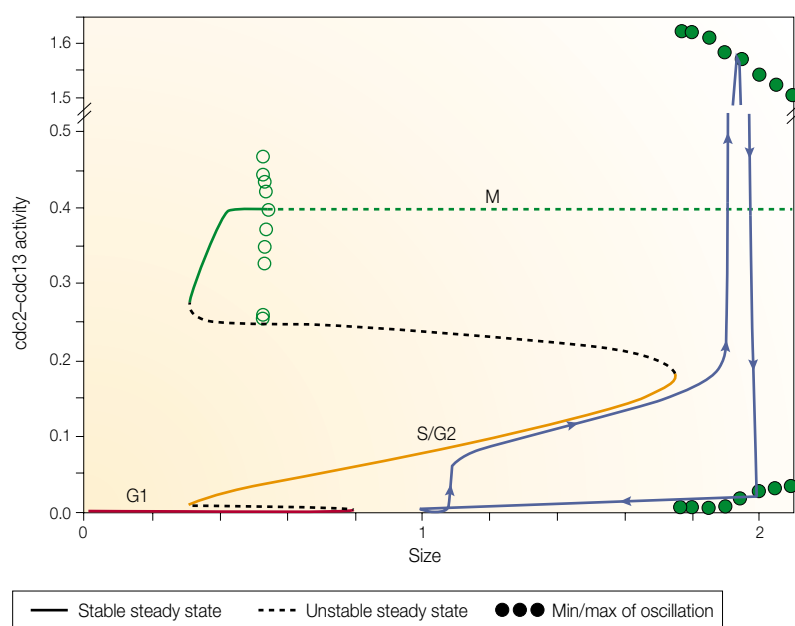

Figure 6 | **Bifurcation diagram for the full cell-cycle control network.** A composite of the three diagrams in FIG. 5. Notice that the full diagram is not a simple sum of the bifurcation diagrams of its modules. In particular, oscillations around the M state are greatly modified in the composite control system. Superimposed on the bifurcation diagram is a 'cell-cycle orbit' (blue line): from the time courses in FIG. 3, we plot size on the abscissa and cdc2–cdc13 activity on the ordinate for representative times between birth and division. Notice that, at small cell size, all three modules support stable steady states. Notice how the cell-cycle orbit follows the attractors of the control system.

Legend: —— Stable steady state - - - - Unstable steady state ●●● Min/max of oscillation

a local attractor of the vector field (analogous to the central G1 dot in FIG. 4). As the cell grows larger, the G1 attractor coalesces with a saddle point of the vector field and disappears (at size ~ 0.8, see FIG. 6). When this happens, the control system makes an irreversible transition to a different stable attractor, with intermediate kinase activity (orange line). In this state, slp1 and ste9 are inactive and rum1 is degraded, so cdc2–cdc13 dimers are abundant, but their activity is hampered by tyrosine phosphorylation of cdc2 by wee1 (BOX 2). We associate this state with the S and G2 phases of the cell cycle, because there is enough kinase activity to trigger DNA synthesis, but not enough to drive the cell into mitosis[43].

With further growth, the S/G2 state is also lost by coalescence with a saddle point (at size = 1.75), and the regulatory network forces an irreversible transition to a stable oscillation around the mitotic state with high kinase activity (wee1 inactive, cdc25 active). As cdc2 activity rises abruptly, the cell enters mitosis, its replicated chromosomes are brought into alignment on the metaphase plate and slp1 is activated. Slp1 induces the separation of sister chromatids and degradation of cdc13. Cdc2 activity drops, triggering nuclear division and resetting the size from 2 to 1. The drop in size moves the molecular regulatory system from the oscillatory region back to a G1-like state.

It is instructive to project the simulated time courses of cell size and cdc2 activity (FIG. 3) onto the bifurcation diagram. The blue line in FIG. 6 traces out this cell-cycle orbit. Notice how, as the cell proceeds through its division cycle, the orbit tries to follow the attractors of the control system. A wild-type fission yeast cell, born at size = 1, finds itself in a pseudo-G1 state (slp1 active, ste9 active, rum1 abundant). But this state is only transitory. As soon as slp1 reverts to its inactive form, the control system is attracted to the stable S/G2 state because the cell is too large to persist in true G1 (slp1 inactive, ste9 active, rum1 abundant). The wild-type cell spends a long time in S/G2, waiting to grow large enough to enter mitosis[44]. After the transition, mitosis happens quickly in fission yeast. As the cell exits mitosis, cdc2 activity drops precipitously, which triggers nuclear and cell division, size drops abruptly from 2 to 1 and the control system returns to the pseudo-G1 state.

Mutant phenotypes confirm the model
In wild-type fission yeast, cell size controls the G2/M transition[44]. In our model, to move from S/G2 to M, a cell must grow large enough to get past the 'nose' of the bifurcation diagram (size = 1.75 in FIG. 6). Cell size at the end of the nose depends sensitively on the expression levels of wee1 and cdc25 in the model[37,45], exactly as in experiments[39,40]. In particular, in *wee1⁻* cells (non-functional wee1 protein), the nose of the S/G2 state disappears; the cell enters mitosis and divides at an abnormally small size, and is then captured by the G1/S module. These mutant cells are now size controlled at the G1/S transition (size = 0.8 in FIG. 6) and divide at about half the size of wild-type cells, exactly as observed[46]. Indeed, the 'wee' phenotype of these mutant cells attracted Paul Nurse's attention to the significance of a trio of genes (*wee1*, *cdc2* and *cdc25*) that provided the first glimpse of the cell-cycle regulatory network in eukaryotes. For this discovery, he received the Nobel Prize for Physiology or Medicine in 2001, together with Leland Hartwell (for the discovery of the cyclin-dependent kinase gene, *CDC28*, in budding yeast) and Tim Hunt (for the discovery of cyclins, in sea urchin embryos). See the 'Milestones in cell division' supplement for further details.

In wild-type cells, a full oscillation of the mitotic module (FIGS 2, 5c) never occurs, because these cells divide and leave the oscillatory region (FIG. 6). However, in *wee1⁻ rum1*[deletion] mutants, both the G1/S and G2/M modules lose their bistable characteristics, and these transitions are no longer responsive to cell size. In this case, the oscillatory character of the mitotic module asserts itself: these mutants divide faster than they grow, becoming progressively smaller until they die[47,48].

Implications and future directions
Kinetic modelling and bifurcation theory provide a precise, mathematical connection between the molecular network that surrounds cyclin-dependent kinase and the classical phases of the cell cycle. Computer simulations of the model are in accord with the physiological properties of wild-type cells and scores of interesting mutants. The theory indicates that the irreversible

transitions of the cell cycle might be consequences of bifurcations in the vector field of the kinetic equations. This suggestion and other predictions of the model have recently been tested in budding yeast by Cross *et al.*[49]. In addition, the theory indicates that the checkpoints of the cell cycle[50,51] might be mechanisms that stabilize certain attractors of the vector field by putting off the bifurcations that normally propel cells through the cycle. For example, problems with DNA replication create a signal that inactivates cdc25 (REF. 52) and activates mik1 (a wee1-like tyrosine kinase)[53], and stretches out the nose of the S/G2 state to a very large size (>> 2). Consequently, a cell with unreplicated DNA cannot leave S/G2 and enter M phase. If the checkpoint mechanism is compromised by certain mutations, cells enter mitosis after a delay[53], presumably because they grow large enough to get past a nose that is not as big as it should be.

These novel conclusions, though implicit in the wiring diagram, come to light only when the molecular information is subjected to the proper scientific analysis. After formulating the network in mathematical terms, its qualitative features can be discovered by the tools of dynamical systems theory, and quantitative results can be computed for comparison with experiments. For instance, our cell-cycle model predicts that, in small cells, all three modules (FIG. 2) support stable steady states (FIG. 6). This prediction might be testable in germinating fission-yeast spores, which are very small[54]. If we could stop these cells from growing (say, by blocking ribosomal RNA synthesis), and then induce them to transcribe extra *cdc13* messenger RNA, we might be able to push small cells prematurely into a stable S/G2 or a stable mitotic state.

Cell-cycle control is a particularly compelling example of the dynamical-systems approach to cell physiology, because cell-cycle transitions are so evidently connected to bifurcations of vector fields (see the references in BOX 3). The same approach has been used to advantage in numerous studies of other molecular regulatory systems (BOX 3). Although much of this work uses nonlinear differential equations and bifurcation analysis, in some cases it is more appropriate to use stochastic equations, Boolean networks, or cellular automata, and different tools from the theory of dynamical systems. But in all cases, the central themes are the same: a dynamical system describes how the network evolves in state space, and these changes determine the physiological behaviour of the cell. This theme is elaborated in several excellent textbooks by Segel[55], Goldbeter[56], Keener and Sneyd[57], and Fall *et al.*[58].

Spontaneous spatial and temporal organization of dynamical systems is, therefore, the unifying principle of the 'last step' of computational molecular biology. Analysis and simulation of mathematical models provides a rigorous way to correlate cell physiology with underlying molecular networks. Experimentalists need to be familiar with the basic ideas that make this correlation possible (vector fields, stability and bifurcations), just as theoreticians, if they are to make a useful contribution to the life sciences, need to know the basic principles of molecular genetics, protein interactions and biochemical regulation. Only when the two communities speak a common language can they collaborate fruitfully on problems of network dynamics and cell physiology.

1. Osguthorpe, D. J. *Ab initio* protein folding. *Curr. Opin. Struct. Biol.* **10**, 146–152 (2000).
2. Baker, D. & Sali, A. Protein structure predictions and structural genomics. *Science* **294**, 93–96 (2001).
3. Kollman, P. A. *et al.* Calculating structures and free energies of complex molecules: combining molecular mechanics and continuum models. *Acc. Chem. Res.* **33**, 889–897 (2000).
4. Wang, W., Donini, O., Reyes, C. M. & Kollman, P. A. Biomolecular simulations: recent developments in force fields, simulations of enzyme catalysis, protein–ligand, protein–protein, and protein–nucleic acid noncovalent interactions. *Annu. Rev. Biophys. Biomol. Struct.* **30**, 211–243 (2001).
5. Hu, X., Ritz, T., Damjanovic, A. & Schulten, K. Pigment organization and transfer of electronic excitation in the photosynthetic unit of purple bacteria. *J. Phys. Chem. B* **101**, 3854–3871 (1997).
6. Elston, T., Wang, H. & Oster, G. Energy transduction in ATP synthase. *Nature* **391**, 510–513 (1998).
7. Chung, S.-H., Allen, T. W., Hoyles, M. & Kuyucak, S. Permeation of ions across the potassium channel: Brownian dynamics studies. *Biophys. J.* **77**, 2517–2533 (1999).
8. Bray, D. Protein molecules as computational elements in living cells. *Nature* **376**, 307–312 (1995).
   This paper presents the case for protein networks as information-processing units in the cell.
9. Weinberg, R. A. The retinoblastoma protein and cell-cycle control. *Cell* **81**, 323–330 (1995).
10. Planas-Silva, M. D. & Weinberg, R. A. The restriction point and control of cell proliferation. *Curr. Opin. Cell Biol.* **9**, 768–772 (1997).
11. Hanahan, D. & Weinberg, R. A. The hallmarks of cancer. *Cell* **100**, 57–70 (2000).
12. Kohn, K. W. Molecular interaction map of the mammalian cell-cycle control and DNA repair systems. *Mol. Biol. Cell* **10**, 2703–2734 (1999).
13. Hasty, J., McMillen, D., Isaacs, F. & Collins, J. J. Computational studies of gene regulatory networks: *in numero* molecular biology. *Nature Rev. Genet.* **2**, 268–279 (2001).
    An excellent, comprehensive review of modelling genetic regulatory systems.
14. Meinhardt, H. Hierarchical inductions of cell states: a model for segmentation in *Drosophila*. *J. Cell Sci.* (Suppl.) **4**, 357–381 (1986).
15. Reinitz, J., Mjolsness, E. & Sharp, D. H. Model for cooperative control of positional information in *Drosophila* by bicoid and maternal hunchback. *J. Exp. Zool.* **271**, 47–56 (1995).
16. McAdams, H. H. & Shapiro, L. Circuit simulation of genetic networks. *Science* **269**, 650–656 (1995).
17. Von Dassow, G., Meir, E., Munro, E. M. & Odell, G. M. The segment polarity network is a robust developmental module. *Nature* **406**, 188–192 (2000).
18. Sanchez, L. & Thieffry, D. A logical analysis of the *Drosophila* gap–gene system. *J. Theor. Biol.* **211**, 115–141 (2001).
19. Tyson, J. J. & Murray, J. D. Cyclic AMP waves during aggregation of *Dictyostelium* amoebae. *Development* **106**, 421–426 (1989).
20. Dupont, G. & Goldbeter, A. Oscillations and waves of cytosolic calcium: insights from theoretical models. *BioEssays* **14**, 485–493 (1992).
21. Gerhardt, M., Schuster, H. & Tyson, J. J. A cellular automaton model of excitable media. *Science* **247**, 1563–1566 (1990).
22. Markus, M. & Hess, B. Isotropic cellular automaton for modelling excitable media. *Nature* **347**, 56–58 (1990).
23. Smolen, P., Baxter, D. A. & Byrne, J. H. Modeling circadian oscillations with interlocking positive and negative feedback loops. *J. Neurosci.* **21**, 6644–6656 (2001).
24. Lema, M. A., Golombek, D. A. & Echave, J. Delay model of the circadian pacemaker. *J. Theor. Biol.* **204**, 565–574 (2000).
25. Mackey, M. C. in *Case Studies in Mathmatical Modelling* (eds Othmer, H. G., Adler, F. R., Lewis, M. A. & Dallon, J. C.) 149–178 (Prentice Hall, New Jersey, 1997).
26. Wilson, H. R. & Cowan, J. D. A mathematical theory of the functional dynamics of cortical and thalamic nervous tissue. *Kybernetik* **13**, 55–80 (1973).
27. Ermentrout, G. B. & Cowan, J. D. A mathematical theory of visual hallucination patterns. *Biol. Cybernet.* **34**, 137–150 (1979).
28. Arkin, A., Ross, J. & McAdams, H. H. Stochastic kinetic analysis of developmental pathway bifurcation in phage λ-infected *Escherichia coli* cells. *Genetics* **149**, 1633–1648 (1998).
29. McAdams, H. H. & Arkin, A. It's a noisy business. *Trends Genet.* **15**, 65–69 (1999).
30. Jacquez, J. A. *Compartmental Analysis in Biology and Medicine* (Elsevier Science, Amsterdam, 1972).
31. Tyson, J. J., Novak, B., Odell, G. M., Chen, K. & Thron, C. D. Chemical kinetic theory as a tool for understanding the regulation of M-phase promoting factor in the cell cycle. *Trends Biochem. Sci.* **21**, 89–96 (1996).
32. Tyson, J. J. & Novak, B. Regulation of the eukaryotic cell cycle: molecular antagonism, hysteresis and irreversible transitions. *J. Theor. Biol.* **210**, 249–263 (2001).
33. Kaplan, D. & Glass, L. *Understanding Nonlinear Dynamics* (Springer, New York, 1995).
34. Strogatz, S. H. *Nonlinear Dynamics and Chaos* (Addison-Wesley Co., Reading, Massachusetts, 1994).
35. Tyson, J. J., Novak, B., Chen, K. C. & Val, J. in *Progress in Cell Cycle Research* (eds Meijer, L., Guidet, S. & Tung, H. Y. L.) 1–8 (Plenum, New York, 1995).
36. Thron, C. D. Bistable biochemical switching and the control of the events of the cell cycle. *Oncogene* **15**, 317–325 (1997).
37. Novak, B. & Tyson, J. J. Quantitative analysis of a

molecular model of mitotic control in fission yeast. *J. Theor. Biol.* **173**, 283–305 (1995).

38. Fantes, P. A. Control of cell size and cycle time in *Schizosaccharomyces pombe*. *J. Cell Sci.* **24**, 51–67 (1977).

39. Russell, P. & Nurse, P. *cdc25*⁺ functions as an inducer in the mitotic control of fission yeast. *Cell* **45**, 145–153 (1986).

40. Russell, P. & Nurse, P. Negative regulation of mitosis by *wee1*⁺, a gene encoding a protein kinase homolog. *Cell* **49**, 559–567 (1987).

41. Nurse, P. Universal control mechanism regulating onset of M phase. *Nature* **344**, 503–508 (1990).

42. Goldbeter, A. A minimal cascade model for the mitotic oscillator involving cyclin and cdc2 kinase. *Proc. Natl Acad. Sci. USA* **88**, 9107–9111 (1991).

43. Stern, B. & Nurse, P. A quantitative model for the cdc2 control of S phase and mitosis in fission yeast. *Trends Genet.* **12**, 345–350 (1996).

44. Fantes, P. & Nurse, P. Control of cell size at division in fission yeast by a growth-modulated size control over nuclear division. *Exp. Cell Res.* **107**, 377–386 (1977).

45. Sveiczer, A., Csikasz-Nagy, A., Gyorffy, B., Tyson, J. J. & Novak, B. Modeling the fission yeast cell cycle: quantized cycle times in *wee1⁻cdc25Δ* mutant cells. *Proc. Natl Acad. Sci. USA* **97**, 7865–7870 (2000).

46. Nurse, P. Genetic control of cell size at cell division in yeast. *Nature* **256**, 547–551 (1975).

47. Moreno, S. & Nurse, P. Regulation of progression through the G1 phase of the cell cycle by the *rum1⁺* gene. *Nature* **367**, 236–242 (1994).

48. Novak, B. & Tyson, J. J. Modeling the control of DNA replication in fission yeast. *Proc. Natl Acad. Sci. USA* **94**, 9147–9152 (1997).

49. Cross, F. R., Archambault, V., Miller, M. & Klovstad, M. Testing a mathematical model for the yeast cell cycle. *Mol. Biol. Cell* (in the press).

50. Hartwell, L. H. & Weinert, T. A. Checkpoints: controls that ensure the order of cell cycle events. *Science* **246**, 629–634 (1989).

51. Rhind, N. & Russell, P. Mitotic DNA damage and replication checkpoints in yeast. *Curr. Opin. Cell Biol.* **10**, 749–758 (1998).

52. Furnari, B., Rhind, N. & Russell, P. Cdc25 mitotic inducer targeted by Chk1 DNA damage checkpoint kinase. *Science* **277**, 1495–1497 (1997).

53. Rhind, N. & Russell, P. Roles of the mitotic inhibitors Wee1 and Mik1 in the G₂ DNA damage and replication checkpoints. *Mol. Cell. Biol.* **21**, 1499–1508 (2001).

54. Nurse, P. & Thuriaux, P. Controls over the timing of DNA replication during the cell cycle of fission yeast. *Exp. Cell Res.* **107**, 365–375 (1977).

55. Segel, L. A. *Mathematical Models in Molecular and Cellular Biology* (Cambridge Univ. Press, Cambridge, 1980).

56. Goldbeter, A. *Biochemical Oscillations and Cellular Rhythms* (Cambridge Univ. Press, Cambridge, 1996).

57. Keener, J. & Sneyd, J. *Mathematical Physiology* (Springer, New York, 1998).

58. Fall, C. P., Marland, E., Wagner, J. M. & Tyson, J. J. *Computational Cell Biology* (Springer, New York, 2002).

59. Fraser, S. E. & Harland, R. M. The molecular metamorphosis of experimental embryology. *Cell* **100**, 41–55 (2000).

60. Nurse, P. A long twentieth century of the cell cycle and beyond. *Cell* **100**, 71–78 (2000).

61. Hartwell, L. H., Hopfield, J. J., Leibler, S. & Murray, A. W. From molecular to modular cell biology. *Nature* **402**, C47–C52 (1999).
    This paper makes a case for modularity in molecular regulatory systems.

62. Butler, D. Computing 2010: from black holes to biology. *Nature* **402**, C67–C70 (1999).

63. Novak, B., Pataki, Z., Ciliberto, A. & Tyson, J. J. Mathematical model of the cell division cycle of fission yeast. *Chaos* **11**, 277–286 (2001).

64. Benito, J., Martin-Castellanos, C. & Moreno, S. Regulation of the G1 phase of the cell cycle by periodic stabilization and degradation of the p25rum1 CDK inhibitor. *EMBO J.* **17**, 482–497 (1998).

65. Blanco, M. A., Sanchez-Diaz, A., De Prada, J. M. & Moreno, S. APC (ste9/srw1) promotes degradation of mitotic cyclins in G1 and is inhibited by cdc2 phosphorylation. *EMBO J.* **19**, 3945–3955 (2000).

66. Yamaguchi, S., Okayama, H. & Nurse, P. Fission yeast Fizzy-related protein srw1p is a G₁-specific promoter of mitotic cyclin B degradation. *EMBO J.* **19**, 3968–3977 (2000).

67. Aligue, R., Wu, L. & Russell, P. Regulation of *Schizosaccharomyces pombe* Wee1 tyrosine kinase. *J. Biol. Chem.* **272**, 13320–13325 (1997).

68. Millar, J. B. A. & Russell, P. The cdc25 M-phase inducer: an unconventional protein phosphatase. *Cell* **68**, 407–410 (1992).

69. Hyver, C. & Le Guyader, H. MPF and cyclin — modeling of the cell-cycle minimum oscillator. *Biosystems* **24**, 85–90 (1990).

70. Norel, R. & Agur, Z. A model for the adjustment of the mitotic clock by cyclin and MPF levels. *Science* **251**, 1076–1078 (1991).

71. Tyson, J. J. Modeling the cell division cycle: cdc2 and cyclin interactions. *Proc. Natl Acad. Sci. USA* **88**, 7328–7332 (1991).

72. Novak, B. & Tyson, J. J. Numerical analysis of a comprehensive model of M-phase control in *Xenopus* oocyte extracts and intact embryos. *J. Cell Sci.* **106**, 1153–1168 (1993).
    The first comprehensive model of cell-cycle regulation, carefully compared with experiments on intact frog embryos and cell-free egg extracts.

73. Marlovits, G., Tyson, C. J., Novak, B. & Tyson, J. J. Modeling M-phase control in *Xenopus* oocyte extracts: the surveillance mechanism for unreplicated DNA. *Biophys. Chem.* **72**, 169–184 (1998).

74. Borisuk, M. T. & Tyson, J. J. Bifurcation analysis of a model of mitotic control in frog eggs. *J. Theor. Biol.* **195**, 69–85 (1998).

75. Novak, B., Csikasz-Nagy, A., Gyorffy, B., Chen, K. & Tyson, J. J. Mathematical model of the fission yeast cell cycle with checkpoint controls at the G1/S, G2/M and metaphase/anaphase transitions. *Biophys. Chem.* **72**, 185–200 (1998).

76. Chen, K. C. *et al.* Kinetic analysis of a molecular model of the budding yeast cell cycle. *Mol. Biol. Cell* **11**, 369–391 (2000).

77. Obeyesekere, M. N., Herbert, J. R. & Zimmerman, S. O. A model of the G1 phase of the cell cycle incorporating cyclinE/cdk2 complex and retinoblastoma protein. *Oncogene* **11**, 1199–1205 (1995).

78. Hatzimanikatis, V., Lee, K. H. & Bailey, J. E. A mathematical description of regulation of the G1–S transition of the mammalian cell cycle. *Biotechnol. Bioeng.* **65**, 631–637 (1999).

79. Aguda, B. D. & Tang, Y. The kinetic origins of the restriction point in the mammalian cell cycle. *Cell Prolif.* **32**, 321–335 (1999).

80. Fell, D. A. *Understanding the Control of Metabolism* (Portland, London, 1996).

81. Schilling, C. H. & Palsson, B. O. Assessment of the metabolic capabilities of *Haemophilus influenzae* Rd through a genome-scale pathway analysis. *J. Theor. Biol.* **203**, 249–283 (2000).

82. Teusink, B. *et al.* Can yeast glycolysis be understood in terms of *in vitro* kinetics of the constituent enzymes? Testing biochemistry. *Eur. J. Biochem.* **267**, 5313–5329 (2000).

83. Martiel, J. L. & Goldbeter, A. A model based on receptor desensitiztion for cyclic-AMP signaling in *Dictyostelium* cells. *Biophys. J.* **52**, 808–828 (1987).

84. De Young, G. W. & Keizer, J. A single-pool inositol 1,4,5-triphosphate-receptor-based model for agonist-stimulated oscillations in Ca²⁺ concentration. *Proc. Natl Acad. Sci. USA* **89**, 9895–9899 (1992).

85. Mahaffy, J. & Zyskind, J. A model for initiation of replication in *Escherichia coli*. *J. Theor. Biol.* **140**, 453–477 (1989).

86. Bray, D., Bourret, R. B. & Simon, M. I. Computer simulation of the phosphorylation cascade controlling bacterial chemotaxis. *Mol. Biol. Cell* **4**, 469–482 (1993).
    A trend-setting analysis of the molecular machinery that controls bacterial locomotion. Computer simulations reproduce the behaviour of more than 30 mutants in which components of the network are deleted or overexpressed.

87. Meinhardt, H. & De Boer, P. A. Pattern formation in *Escherichia coli*: a model for the pole-to-pole oscillation of MIN proteins and the localization of the division site. *Proc. Natl Acad. Sci. USA* (in the press).

88. Bertram, R., Butte, M. J., Kiemel, T. & Sherman, A. Topological and phenomenological classification of bursting oscillations. *Bull. Math. Biol.* **57**, 413–439 (1995).

89. Izhikevich, E. M. Synchronization of elliptic bursters. *Soc. Ind. Appl. Math. Rev.* **43**, 315–344 (2001).

90. Segel, L. A., Goldbeter, A., Devreotes, P. N. & Knox, B. E. A mechanism for exact sensory adaptation based on receptor modification. *J. Theor. Biol.* **120**, 151–179 (1986).

91. Barkai, N. & Leibler, S. Robustness in simple biochemical networks. *Nature* **387**, 913–917 (1997).

92. Peskin, C. S., Odell, G. M. & Oster, G. F. Cellular motions and thermal fluctuations: the Brownian ratchet. *Biophys. J.* **65**, 316–324 (1993).

93. Gueron, S. & Levit-Gurevich, K. A three-dimensional model for ciliary motion based on the internal 9+2 structure. *Proc. R. Soc. Lond.* B **268**, 599–607 (2001).

94. Endy, D., You, L., Yin, J. & Molineux, I. J. Computation, prediction, and experimental tests of fitness for bacteriophage T7 mutants with permuted genomes. *Proc. Natl Acad. Sci. USA* **97**, 5375–5380 (2000).

95. Goldbeter, A. A model for circadian oscillations in *Drosophila* period protein (PER). *Proc. R. Soc. Lond.* B **261**, 319–324 (1995).

96. Leloup, J. C. & Goldbeter, A. A model for circadian rhythms in *Drosophila* incorporating the formation of a complex between the PER and TIM proteins. *J. Biol. Rhythms* **13**, 70–87 (1998).

97. Tyson, J. J., Hong, C. I., Thron, C. D. & Novak, B. A simple model of circadian rhythms based on dimerization and proteolysis of PER and TIM. *Biophys. J.* **77**, 2411–2417 (1999).

98. Sharp, D. H. & Reinitz, J. Prediction of mutant expression patterns using gene circuits. *Biosystems* **47**, 79–90 (1998).

99. Savageau, M. A. Design of molecular control mechanisms and the demand for gene expression. *Proc. Natl Acad. Sci. USA* **74**, 5647–5651 (1977).
    An early and excellent application of dynamical reasoning to bacterial cell physiology.

100. Keller, A. D. Model genetic circuits encoding autoregulatory transcription factors. *J. Theor. Biol.* **172**, 169–185 (1995).

101. Gardner, T. S., Cantor, C. R. & Collins, J. J. Construction of a genetic toggle switch in *Escherichia coli*. *Nature* **403**, 339–342 (2000).
    A genetic network, artificially engineered in bacteria, confirms the predictions of mathematical models.

102. Goodwin, B. C. An entrainment model for timed enzyme synthesis in bacteria. *Nature* **209**, 479–481 (1966).

103. Bliss, R. D., Painter, R. P. & Marr, A. G. Role of feedback inhibition in stabilizing the classical operon. *J. Theor. Biol.* **97**, 177–193 (1982).

104. Elowitz, M. B. & Leibler, S. A synthetic oscillatory network of transcriptional regulators. *Nature* **403**, 335–338 (2000).

105. Levchenko, A., Bruck, J. & Sternberg, P. W. Scaffold proteins may biphasically affect the levels of mitogen-activated protein kinase signaling and reduce its threshold properties. *Proc. Natl Acad. Sci. USA* **97**, 5818–5823 (2000).

106. Ferrell, J. E. Jr & Xiong, W. Bistability in cell signaling: how to make continuous processes discontinuous and reversible processes irreversible. *Chaos* **11**, 227–236 (2001).

107. Asthagiri, A. R. & Lauffenburger, D. A. A computational study of feedback effects on signal dynamics in a mitogen-activated protein kinase (MAPK) pathway model. *Biotechnol. Prog.* **17**, 227–239 (2001).

108. Fussenegger, M., Bailey, J. E. & Varner, J. A mathematical model of caspase function in apoptosis. *Nature Biotechnol.* **18**, 768–774 (2000).

🌐 Online links

DATABASES
The following terms in this article are linked online to:
cdc2 | cdc13 | cdc25 | *CDC28* | slp1 | ste9 | wee1

FURTHER INFORMATION
Berkeley Madonna: http://www.berkeleymadonna.com/
Cell cycle: http://www.ultranet.com/~jkimball/BiologyPages/C/CellCycle.html
E-CELL: http://www.e-cell.org
Encyclopedia of Life Sciences: http://www.els.net
Cell cycle
GEPASI: http://www.gepasi.org/
Kohn's interaction maps:
http://discover.nci.nih.gov/kohnk/interaction_maps.html
Milestones in cell division: www.nature.com/celldivision
Molecular wiring diagrams: www.biocarta.com
Novak lab: http://cellcycle.mkt.bme.hu
Saccharomyces **genome database:** http://genome-www.stanford.edu/Saccharomyces
Virtual Cell: http://www.nrcam.uchc.edu/
XPPAUT: http://www.pitt.edu/~phase/
Yeast proteome database: http://www.proteome.com/databases/YPD/YPDsearch-long.html
Access to this interactive links box is free online.